

RESEARCH PAPER



Mechanistic insight into the induction of cellular immune responses by encapsulated and admixed archaeosome-based vaccine formulations

Gerard Agbayani^a, Yimei Jia^a, Bassel Akache^a, Vandana Chandan^a, Umar Iqbal^a, Felicity C. Stark^a, Lise Deschatelets^a, Edmond Lam^b, Usha D. Hemraz^b, Sophie Régnier^b, Lakshmi Krishnan^a, and Michael J. McCluskie^a 

^aHuman Health Therapeutics, National Research Council Canada, Ottawa, ON, Canada; ^bAquatic and Crop Resource Development, National Research Council Canada, Montreal, QC, Canada

ABSTRACT

Archaeosomes are liposomes formulated using total polar lipids (TPLs) or semi-synthetic glycolipids derived from archaea. Conventional archaeosomes with entrapped antigen exhibit robust adjuvant activity as demonstrated by increased antigen-specific humoral and cell-mediated responses and enhanced protective immunity in various murine infection and cancer models. However, antigen entrapment efficiency can vary greatly resulting in antigen loss during formulation and variable antigen:lipid ratios. In order to circumvent this, we recently developed an admixed archaeosome formulation composed of a single semi-synthetic archaeal lipid (SLA, sulfated lactosylarchaeol) which can induce similarly robust adjuvant activity as an encapsulated formulation. Herein, we evaluate and compare the mechanisms involved in the induction of early innate and antigen-specific responses by both admixed (Adm) and encapsulated (Enc) SLA archaeosomes. We demonstrate that both archaeosome formulations result in increased immune cell infiltration, enhanced antigen retention at injection site and increased antigen uptake by antigen-presenting cells and other immune cell types, including neutrophils and monocytes following intramuscular injection to mice using ovalbumin as a model antigen. *In vitro* studies demonstrate SLA in either formulation is preferentially taken up by macrophages. Although the encapsulated formulation was better able to induce antigen-specific CD8⁺ T cell activation by dendritic cells *in vitro*, both encapsulated and admixed formulations gave equivalently enhanced protection from tumor challenge when tested *in vivo* using a B16-OVA melanoma model. Despite some differences in the immunostimulatory profile relative to the SLA (Enc) formulation, SLA (Adm) induces strong *in vivo* immunogenicity and efficacy, while offering an ease of formulation.

ARTICLE HISTORY

Received 20 April 2020
Revised 2 June 2020
Accepted 21 June 2020

KEYWORDS

Archaeosome; adjuvant; sulfated lactosyl archaeol; SLA; archaeol; glycolipid; vaccine

Introduction

The hallmark of a successful vaccine is the induction of long-lasting protective responses with minimal risk of local or systemic adverse effects. With subunit vaccines that contain only specific antigen(s) of the target pathogen, the quality and quantity of these protective responses, typically measured by antigen-specific antibody and T-cell responses, are largely influenced by innate immune responses initiated by adjuvants at the injection site.¹ Among the key, early innate immune responses are cytokine and chemokine production, immune cell infiltration and activation, and cellular uptake of antigen.^{1–4} Enhanced production of cytokines and chemokines creates a local inflammatory milieu that leads to the activation and recruitment of innate and adaptive immune cells to the injection site.² This in turn results in enhanced antigen uptake by infiltrating and/or tissue-resident antigen-presenting cells (APCs) which home to draining lymph nodes (LNs) and present vaccine antigens to T cells leading to the induction of antigen-specific effector CD8⁺ T cell responses and B cell-mediated antibody production.² Therefore, adjuvants can impact vaccine effectiveness by bridging critical innate and

adaptive immune responses toward the development of long-lasting protective immunity. A better understanding of the mechanism of action of adjuvants can ultimately help with the rational design of vaccines.

Liposomes are increasingly being utilized in adjuvant formulations, due to their versatility to incorporate a variety of cargo and their ability to initiate antigen-specific cellular responses through the delivery of entrapped antigen and/or adjuvant to the intracellular compartment.⁴ Archaeosomes are liposomes that are traditionally comprised of total polar lipids (TPLs) derived from Archaeobacteria, such as *Methanobrevibacter smithii* (MS), or semi-synthetic glycolipids. The use of archaeosomes as adjuvants presents several advantages over conventional liposomes, particularly high thermal and pH stability, enhanced immunostimulatory properties and reduced proton permeability.⁵ We have previously shown that archaeosomes are highly effective adjuvants to numerous antigens, capable of inducing strong humoral and cell-mediated immune responses and protective immunity in multiple models of murine infection and cancer.^{3,5–11} However, traditional archaeosome formulations were composed of multiple glycolipids making characterization and formulation reproducibility challenging. To simplify

CONTACT Michael J. McCluskie  Michael.McCluskie@nrc-cnrc.gc.ca  Human Health Therapeutics, National Research Council Canada, Ottawa, ON K1A 0R6, Canada

 Supplemental data for this article can be accessed on the [publisher's website](#).

© 2020 The Author(s). Published with license by Taylor & Francis Group, LLC.

This is an Open Access article distributed under the terms of the Creative Commons Attribution-NonCommercial-NoDerivatives License (<http://creativecommons.org/licenses/by-nc-nd/4.0/>), which permits non-commercial re-use, distribution, and reproduction in any medium, provided the original work is properly cited, and is not altered, transformed, or built upon in any way.

formulation, we recently developed an archaeosome comprised of a single glycolipid, sulfated lactosylarchaeol (SLA; 6'-sulfate- β -D-Galp-(1,4)- β -D-Glcp-(1,1)-archaeol), which we have shown can induce strong cellular and humoral responses when used to entrap multiple antigens, such as ovalbumin (OVA), hepatitis B surface antigen (HBsAg), influenza hemagglutinin (HA) and hepatitis C virus (HCV) envelope glycoproteins.^{6,7,10,12–14} SLA archaeosomes are capable of inducing similar long-term, protective cellular and humoral responses as traditional multi-lipid archaeosome formulations with minimal toxicity.^{3,8} Furthermore, SLA archaeosomes have been shown to induce equivalent or increased cytokine/chemokine and antigen-specific antibody and CD8⁺ T cell responses when compared to other established adjuvants, including aluminum hydroxide, TLR3/4/9 agonists, oil-in-water and water-in-oil emulsions.⁶

While initially used to deliver encapsulated antigen, SLA archaeosomes were equally able to induce antigen-specific responses when simply admixed with various antigens.^{7,10,15} Whereas the traditional encapsulated (Enc) archaeosome formulations have variable antigen entrapment efficiency (5–40%), leading to high antigen loss during formulation as well as batch-to-batch differences in archaeal lipid to antigen ratios,^{7,16,17} the admixed (Adm) archaeosome formulation has no antigen loss during production and is highly reproducible while maintaining strong adjuvanticity. The adjuvanticity associated with traditional-encapsulated archaeosome formulations was previously shown to be due to their capacity to deliver encapsulated antigens to APCs followed by processing by a classical MHC class I pathway.¹⁸ Cellular uptake of MS TPL archaeosomes was shown to occur through endocytosis upon recognition of phosphoserine head groups on the archaeosome surface by phosphatidylserine (PS) receptors expressed by APCs.^{18,19} Due to the lack of phosphoserine head groups on SLA archaeosomes, differences in ligand-receptor engagement and subsequent immune activation mechanisms can be expected when compared to traditional archaeosomes.^{18,19} Furthermore, it is possible that SLA archaeosomes in an admixed formulation rely on an alternate MHC class I processing pathway to induce the robust antigen-specific responses observed to date with multiple antigens, given that the antigen is not physically located within the archaeosomes.⁷ Herein, to better understand the mechanisms of action behind the activity of the archaeosome formulations, we compared the effects of two different SLA archaeosome formulations, namely admixed (Adm) and encapsulated (Enc), on immune cell infiltration, antigen biodistribution and cytokine expression at the vaccine injection site in mice. We also evaluated the capacity of SLA formulations to induce cytokine and antigen-specific CD8⁺ T cell responses *in vitro*, as well as modulating mouse survival using the B16-OVA mouse melanoma model.

Materials and methods

Mice

C57BL/6 wild-type and C57BL/6 albino mice (6–8 weeks of age) were purchased from Charles River (Saint-Constant, QC,

Canada). CD45.1⁺CD45.2⁺ OT-1 TCR transgenic mice on the C57BL/6 background were generated by mating OT-1 males (CD45.1⁻CD45.2⁺) with B6. SJL-*Ptprc^a Pepc^b*/BoyJ (CD45.1⁺CD45.2⁻) females, which are both sourced from Jackson Laboratory (Bar Harbor, ME, USA).²⁰ Mice were maintained at the National Research Council (NRC) Canada small animal facility in Ottawa, Canada. The study was performed in accordance with the guidelines of the Canadian Council on Animal Care and animal use protocols 2016.08 and 2016.02 approved by the NRC Human Health Therapeutics Animal Care Committee in Ottawa, Canada.

Vaccine preparations

SLA archaeosomes were prepared according to the thin-film method, as described previously.⁷ Briefly, SLA lipid dissolved in chloroform/methanol was dried under N₂ gas with mild heating to form a thin film of lipid layer. For the preparation of the empty archaeosomes, lipid film was hydrated in Milli-Q water without protein antigen. Ovalbumin antigen (OVA; type VI, Sigma-Aldrich, Oakville, ON, Canada) solution (in desired amount to maintain a specific antigen:lipid ratio) was later added to the pre-formed sized empty archaeosomes. Endotoxin levels for OVA were determined to be below 0.1 EU/ μ g using the Endosafe[®] PTS[™] kit (Charles River Laboratories Inc., Charleston, SC). The admixed formulation was prepared by simply combining the OVA and archaeosome solutions together immediately prior to immunization, followed by brief vortexing. For preparation of encapsulated formulation, lipid film was hydrated with ovalbumin solution followed with ultracentrifugation to remove free OVA. Pellet was washed twice with pyrogen-free water and re-suspended in PBS buffer to desired volume. Sonication was applied to reduce particle size. Protein content was determined in the encapsulated formulation by SDS-PAGE. When administered *in vivo*, the antigen dose was fixed to 10–20 μ g of OVA per injection. With the admixed formulation, the SLA dose was fixed at 1 mg per vaccine dose. Due to the variability inherent with the manufacturing of the encapsulated formulation, the quantity of SLA administered per dose in the separate experiments described below was variable (i.e. 0.2–1 mg). However, all batches fell within our previously established parameters shown to generate strong antigen-specific responses.^{6,7,9,10}

Cellular trafficking and antigen uptake

The OVA antigen (Hyglos GmbH, Bernried am Starnberger See, Germany) was labeled with Alexa Fluor[™] 647-NHS ester (Thermo Fisher Scientific, Pittsburgh, PA, USA) to generate OVA-AF647, as described previously.³ A total of 20 μ g OVA-AF647 in 50 μ L PBS (alone, with SLA (Enc) or SLA (Adm)) was injected intramuscularly (i.m.) into the left tibialis anterior (TA) muscle of C57BL/6 mice. The SLA (Enc) formulation contained 238 μ g of SLA lipid per dose. Negative control mice received 50 μ L PBS i.m. into the left TA muscle. At days 1 and 3 post-injection, TA muscles, inguinal and popliteal LNs were harvested in R10 complete medium (RPMI 1640 with 10% heat-inactivated fetal bovine serum, 1% penicillin/streptomycin, 1% glutamine and 55 μ M 2-mercaptoethanol) (Thermo Fisher Scientific) to

obtain single-cell suspensions. TA muscles were minced with surgical scissors on a 100 mm x 15 mm non-tissue culture-treated petri dish containing filter-sterilized 0.2% collagenase type IV (Worthington Biochemical Corporation, Lakewood, NJ, USA) and 2% heat-inactivated fetal bovine serum in 1x Hank's Balanced Salt Solution. Minced TA muscles were transferred to 15 mL Falcon tubes and incubated in a shaking incubator for 1 h at 37°C and 100 rpm. Cells were then centrifuged at 500 × g for 5 min at 4°C and resuspended in R10 complete medium. In contrast, inguinal and popliteal LNs were mashed between two sterilized glass slides and placed back in R10 complete medium. Tissue homogenates from TA muscles and pooled inguinal and popliteal LNs were then passed through 100 µm cell strainer to obtain a single-cell suspension prior to live cell counting using a Cellometer Auto 2000 cell viability counter (Nexcelom Bioscience, Lawrence, MA, USA).

Cellular trafficking and antigen uptake were evaluated through flow cytometry. Cells were centrifuged and resuspended in 1× phosphate-buffered saline (PBS) containing 1:100 concentration of LIVE/DEAD™ Fixable Blue Dead Cell Stain (Invitrogen, Carlsbad, CA, USA) for 20 min at 4°C in the dark. Afterwards, cells were centrifuged and resuspended in PBS containing 2% heat-inactivated fetal bovine serum, 3 mM EDTA (staining buffer) and unconjugated anti-CD16/CD32 (FcγRIII/II) (Fc block) antibody produced in-house for 10 min at 4°C. Cells were then stained with the following fluorochrome-conjugated antibodies for 30 min at 4°C in the dark: CD45 (30-F11), CD11b (M1/70), Ly-6G (1A8), CD11c (HL3), CD45 R/B220 (RA3-6B2), CD8a (53-6.7) (BD Biosciences, Mississauga, ON, Canada); F4/80 (BM8) and Ly-6C (HK1.4) (BioLegend, San Diego, CA, USA). Cells were washed with PBS and centrifuged at 500 × g for 5 min at 4°C. After removing the supernatant, cells were fixed for 15 min at 4°C in the dark using Cytifix™ Fixation Buffer (BD Biosciences). Lastly, fixed cells were washed and resuspended in staining buffer prior to acquisition on the BD LSR Fortessa™ flow cytometer. Flow cytometry data were analyzed using FlowJo® 10 (BD Biosciences) software. Major live immune cell populations were identified according to cell-surface marker expression, as described previously.³

***In vivo* biodistribution of antigen**

OVA antigen was labeled with CF770-NHS ester (Biotium Inc. Fremont, CA, USA) using methods recommended by the manufacturer. Briefly, CF770-NHS ester powders were solubilized in DMSO to create a 31.38 mg/ml solution. To the protein antigen in PBS, pH 7.4, 10% (v/v) carbonate buffer, pH 9.3 and 5× molar excess of CF770-NHS ester were added in separate tubes while mixing. Reactions were then incubated at room temperature for 2 hr with slow mixing. Unreacted dye was removed using an Amicon® Ultra-4 Centrifugal Filter Unit (Sigma-Aldrich) with a 10 k cutoff membrane and the labeled protein antigen was resuspended in PBS, pH 7.4. Labeling was optimized to achieve a dye/protein ratio of approximately 2.

The *in vivo* biodistribution of CF770-labeled OVA, CF770-labeled OVA entrapped in SLA archaeosome, or CF770-labeled OVA admixed with SLA archaeosome following a single i.m. administration were assessed in C57BL/6 albino female mice

(n = 4 per group). A 20 µg dose of CF770-labeled OVA (alone, with SLA (Enc) or SLA (Adm)) was injected into the left T. A. muscle in a volume of 50 µL per injection. The SLA (Enc) formulation contained 638 µg of SLA lipid per dose. Animals were subjected to *in vivo* imaging studies using an IVIS Kinetic small animal imager (Perkin Elmer, Waltham, MA, USA). Animals were imaged at pre-scan, 10 min, 1.5 h, 3 h, 6 h, 24 h, 48 h, 72 h, 96 h and 168 h. Total fluorescence intensity data were determined from select regions of interest (ROI) using the Living Image 4.1 software (Perkin Elmer).

Muscle processing for cytokine/chemokine analysis

C57BL/6 mice were immunized by i.m. injection into the left TA (50 µL) with 20 µg OVA-AF647 alone, with SLA (Enc) or SLA (Adm). The SLA (Enc) formulation contained 238 µg of SLA lipid per dose. TA muscles were collected and processed at 6 h post-injection. Briefly, TA muscles were flash-frozen on dry ice and resuspended in T-PER™ tissue protein extraction reagent (Thermo Scientific™, Waltham, MA, USA) containing cComplete™, Mini, EDTA-free Protease Inhibitor Cocktail (Roche, Mannheim, Germany). TA muscles were homogenized using the Precellys Evolution homogenizer (Bertin Technologies, Versailles, France) at 6,500 rpm, 3 × 10 s cycle and 10 s pause. Tissue lysates were collected after centrifugation at 15,000 rpm for 10 min at 4°C. Total protein concentration per muscle was determined using the Pierce™ BCA Protein Assay Kit (Thermo Fisher Scientific, Pittsburgh, PA, USA).

Mouse tumor challenge

B16 melanoma tumor cell line expressing plasmid-derived full-length ovalbumin (B16-OVA) was obtained from Dr. E. Lord (University of Rochester, Rochester, NY, USA). B16-OVA cells were cultured in R10 complete medium. C57BL/6 mice were first immunized by i.m. injection into the left TA with the following formulations in 50 µL PBS: 10 µg OVA alone, with SLA (Enc) and SLA (Adm). The SLA (Enc) formulation contained 1000 µg of SLA lipid per dose. At 3 weeks post-immunization, solid tumors were induced by injecting 5 × 10⁵ B16-OVA cells subcutaneously (s.c.) in the mid-dorsal flank. Detectable solid tumors were measured with a digital caliper (Mitutoyo 500–196, Aurora, IL, USA) every 1–4 days starting from 5 days post-tumor cell injection, with monitoring frequency increased as the mice approached the endpoints described below. Mice were euthanized upon reaching experimental and humane endpoints. Experimental endpoints included tumor volume reaching 2000 mm³ and/or tumor ulceration with visible liquid discharge or bleeding. Tumor volume was calculated using the formula (L x W x W)/2, where L is tumor length and W is tumor width. Signs of clinical illness such as piloerection, lack of grooming, altered activity level, respiratory distress, hunched posture and morbidity were designated as humane endpoints. As administration of adjuvant without antigen has not induced significant anti-tumor responses in previous studies, we did not include this control in the current study to minimize the unnecessary use of animals.

Generation of BMDMs and BMDCs

Tibias and femurs from C57BL/6 mice were harvested and the interior flushed with R10 complete medium. Cells were passed through 100 μm nylon cell strainer to obtain a single-cell suspension. BMDMs were generated *in vitro* by culturing BM cells on a 100 mm x 15 mm non-tissue culture-treated polystyrene petri dish with R10 complete medium and 10 ng/mL recombinant mouse M-CSF (R&D Systems, Minneapolis, MN, USA) at 37°C and 5% CO₂ in the incubator. BMDCs were generated *in vitro* by culturing cells in a T-25 flask containing R10 complete medium and 10 ng/mL recombinant mouse GM-CSF (R&D Systems) at 37°C and 5% CO₂ in the incubator. Cell culture media was replaced with fresh R10 and either 10 ng/mL M-CSF or GM-CSF for BMDMs and BMDCs, respectively, on days 2 and 4 of culture. BMDMs and BMDCs were collected at day 6 of culture. Briefly, BMDMs were first washed with pre-warmed PBS prior to incubation in PBS at 37°C and 5% CO₂. After 5 to 7 min, cells were lifted from the plate using a Falcon® cell scraper with 18 cm handle and 1.8 cm blade (BD). In contrast, BMDCs were obtained by pipetting up and down several times and collecting the non-adherent and loosely adherent fractions of the cell culture. BMDMs and BMDCs were counted using the Cellometer Auto 2000 cell counter (Nexcelom Bioscience) prior to plating for subsequent assays. BMDM and BMDC purity were routinely determined to be $\geq 90\%$ through flow cytometric analysis of CD11c⁻ F4/80⁺ and CD11c⁺ F4/80⁻ cell populations, respectively.

Phagocytosis assay

BMDMs and BMDCs were plated onto a 96-well flat-bottom plate at 1×10^4 cells per well. Cells were given at least 30 min to adhere to the plates before adding any treatments. Cell supernatants were removed after centrifugation at 500 \times g for 5 min. As negative controls for phagocytosis, duplicate wells of BMDMs and BMDCs were pre-incubated with 10 μM cytochalasin D (cytoD) ready-made solution (from *Zygosporium mansonii*) (Sigma-Aldrich) in R10 complete medium for 1 hr at 37°C and 5% CO₂ in the incubator. R10 complete medium was added to the wells that did not receive cytoD.

SLA liposomes were stained with rhodamine DHPE labeled with red-fluorescent fluorophore (Fisher Scientific, Toronto, ON, Canada) at a lipid-to-dye ratio of 200:1. A total of 1 $\mu\text{g}/\text{mL}$ OVA formulated with 170 $\mu\text{g}/\text{mL}$ SLA (Adm and Enc) were added to duplicate wells. SLA concentrations were optimized for minimal background fluorescence upon live-cell monitoring using the IncuCyte® S3 system (Essen BioScience, Ann Arbor, Michigan, USA). Addition of SLA formulations to phagocytosis negative control wells reduced the final concentration of cytoD to 5 μM . Images per well from two technical replicates were taken every 30 min for up to 6 h. Cellular uptake of SLA was measured as the total red integrated intensity (red calibrated unit [RCU] \times μm^2 per image) using the IncuCyte S3 2018C software.

CD8⁺ T cell activation assay

BMDMs were plated onto a 96-well non-tissue culture-treated U-bottom plate at 1×10^5 cells per well for easy detachment of adherent cells for downstream analysis. BMDCs were plated

onto a 96-well tissue culture-treated U-bottom plate at 1×10^5 cells per well. Cells were given at least 30 min at 37°C and 5% CO₂ in the incubator to adhere to the plates before adding any treatments. A total of 10 $\mu\text{g}/\text{mL}$ OVA was added to duplicate well alone or formulated with 850 $\mu\text{g}/\text{mL}$ SLA (Adm and Enc). In addition, cells were stimulated with SLA without antigen at a similar concentration to the OVA containing formulations. Cells were incubated overnight at 37°C and 5% CO₂ in the incubator. Unbound antigen was removed by centrifuging cells at 500 \times g for 5 min and washing twice in R10 complete medium. Splensens from OT-1 mice were harvested and processed to obtain a single-cell suspension. A total of 1×10^5 OT-1 splenocytes were then added to duplicate wells to obtain a 1:1 ratio of OT-1 splenocytes to BMDMs or BMDCs. OT-1 splenocytes that were stimulated with Concanavalin A from *Canavalia ensiformis* (ConA) (Sigma-Aldrich) served as positive controls (data not shown). In contrast, unstimulated OT-1 cells and BMDM or BMDC + OT-1 co-cultures served as negative controls. The following morning, cells were incubated with GolgiPlug™ Protein Transport Inhibitor (BD Biosciences) for 4 h prior to collection and processing for flow cytometry staining. BMDM:OT-1 co-cultures were first washed with PBS and centrifuged at 500 \times g for 5 min to remove residual heat-inactivated fetal bovine serum. Cells were then incubated in PBS for 5 to 7 min at 37°C and 5% CO₂ in the incubator. The non-adherent and adherent fractions were collected by pipetting the cells up and down several times. In contrast, BMDC:OT-1 co-cultures were simply pipetted up and down several times to collect the cells. Both co-cultures were resuspended in PBS containing 1:100 concentration of LIVE/DEAD™ Fixable Blue Dead Cell Stain (Invitrogen) for 20 min at 4°C in the dark. Cells were washed with PBS, centrifuged and resuspended in staining buffer prior to incubation with Fc block for 10 min at 4°C. Afterwards, cells were stained with the following fluorochrome-conjugated antibodies for 30 min at 4°C in the dark: CD45 (30-F11), TCR- β (H57-597), CD8a (53-6.7), CD69 (H1.2F3), CD44 (IM7) (BD Biosciences). Cells were washed with staining buffer, centrifuged and resuspended in Cytofix/Cytoperm™ (BD Biosciences) for 10 min at 4°C in the dark. Cells were washed twice and resuspended in 1X Perm/Wash™ buffer (BD Biosciences) prior to staining with IFN- γ (XMG1.2) (BD Biosciences) for 15 min at RT in the dark. Lastly, cells were washed and resuspended in staining buffer before acquisition on the BD LSR Fortessa™. CD8⁺ T cell phenotype and functionality were analyzed using FlowJo® 10 (BD Biosciences) software.

Cytokine/chemokine analysis

The expression levels of IL-5, IL-6, IL-10, GM-CSF, G-CSF, TNF- α cytokines and IP-10, KC, MCP-1, MIP-1 α , MIP-1 β , MIP-2 chemokines in TA muscle homogenates and cell culture supernatants were measured using a custom MILLIPLEX® Mouse Analyte kit (Millipore, Billerica, MA, USA). Briefly, 25 μL of sample was incubated overnight with 25 μL antibody-immobilized cytokine bead mix per well on a 96-well MAG-PLATE at 4°C with shaking in the dark. Samples were washed twice with wash buffer and incubated at RT in the dark with detection antibodies for 1 h, followed by streptavidin-

phycoerythrin for 30 min. Lastly, samples were washed twice and resuspended in 150 μ L wash buffer prior to acquisition on the Luminex MAGPIX[®] instrument (Millipore Sigma, Burlington, MA, USA). Cytokine expression levels were analyzed using the Milliplex[™] Analyst software (MilliporeSigma).

Statistical analysis

All statistical analyses were performed using GraphPad[®] Prism 8 software. Data were presented as mean \pm SEM or mean, as indicated in the figure legends. Statistical significance of the difference between three or more groups was determined using one-way or two-way ANOVA followed by Tukey's multiple comparisons test. Survival curves were analyzed using Gehan-Breslow-Wilcoxon test. *P* values of $<.05$ were considered statistically significant. *: $p < .05$, **: $p < .01$, ***: $p < .001$, ****: $p < .0001$.

Results

SLA (Enc) and (Adm) formulations promote early immune cell recruitment to the injection site, enhance antigen uptake and trafficking to draining lymph nodes

To determine whether SLA archaeosome formulation method (Enc or Adm) would affect the recruitment of immune cells to the injection site, antigen uptake at the injection site and trafficking to draining LNs, we used a fluorescent dye conjugated to OVA (OVA-AF647), Cellometer live cell counting and multi-color flow cytometry to identify number and composition of antigen-positive cells in the injected muscle and draining LNs. Both archaeosome formulations induced immune cell infiltration into the muscle and increased antigen uptake. For example, at day one, mice injected with SLA (Enc) OVA-AF647 showed a \sim 3-fold increase in total live cell numbers in the muscles compared to mice that received OVA-AF647 (mean \pm SEM; 250,000 \pm 55,571 vs. 82,840 \pm 7,901) (Table 1). This result correlated with increased numbers of macrophages (64,249 \pm 13,745 vs. 15,628 \pm 1,183), DCs (41,463 \pm 9,428 vs. 9,650 \pm 968), neutrophils (39,223 \pm 6,515 vs. 7,292 \pm 1,146), CD8⁺ T cells (26,975 \pm 7,387 vs. 10,144 \pm 1,614) and monocytes (26,007 \pm 6,311 vs. 10,696 \pm 1,346) relative to mean cell numbers

with OVA-AF647 alone (Table 1). Mice injected with SLA (Enc) OVA-AF647 also exhibited significantly elevated numbers of OVA-AF647⁺ macrophages (52,699 \pm 11,249 vs 8,770 \pm 1,243), neutrophils (32,364 \pm 5,318 vs 3,395 \pm 763), DCs (22,648 \pm 5,249 vs 4,851 \pm 437), CD8⁺ T cells (18,833 \pm 4,526 vs 2,127 \pm 563) and monocytes (16,386 \pm 3,870 vs 1,795 \pm 346) in the injected muscle compared to mean cell numbers with OVA-AF647 alone. In contrast, mice that received SLA (Adm) OVA-AF647 exhibited an increase only in the number of neutrophils in the muscles compared to OVA-AF647 alone (53,430 \pm 12,009 vs. 7,292 \pm 1,146, respectively) at day 1 (Table 1). However, by day 3 post-injection, total live cell numbers in the injected muscle had increased \sim 5-fold with SLA (Adm) treatment compared to OVA-AF647 (481,800 \pm 91,409 vs. 84,160 \pm 10,636, respectively) (Table 1). This result correlated with significantly enhanced levels of OVA-AF647⁺ macrophages (66,193 \pm 14,231 vs. 8,535 \pm 2,186), CD8⁺ T cells (31,244 \pm 5,809 vs. 359 \pm 118), DCs (21,382 \pm 3,673 vs. 8,647 \pm 1,758), monocytes (14,936 \pm 5,132 vs. 3,182 \pm 1,259) and neutrophils (11,719 \pm 846 vs. 199 \pm 64) in the injected muscle relative to mean cell numbers with OVA-AF647 alone (Figure 1B).

Both archaeosome formulations also appeared to increase the number of immune cells and trafficking of antigen to draining LNs. For example, mice injected with SLA (Adm) or SLA (Enc) had \sim 2- to 5-fold higher total live cell numbers relative to mice that received OVA-AF647 alone at both days 1 and 3 post-injection (Table 2). At day 1 post-injection, OVA-AF647⁺ cells in pooled LNs from both SLA (Enc) and (Adm) groups were mainly comprised of B cells, DCs, CD8⁺ T cells, macrophages and monocytes (Figure 1A). OVA-AF647⁺ cell numbers in pooled LNs were drastically reduced in both groups from day 1 to day 3 post-injection (Figure 1A,B). Taken together, SLA Enc and Adm formulations are capable of inducing robust immune cell recruitment and increasing antigen uptake in the injected muscle and trafficking to local LNs.

SLA (Enc) and (Adm) formulations enhance antigen retention at injection site

The effect of SLA archaeosome formulation method (Enc or Adm) on antigen retention and distribution following i.m.

Table 1. Numbers of immune cell types in the left TA muscles of mice injected i.m. with SLA (Enc) and (Adm).

Time Point (Day)	Immune Cell Type	PBS		OVA-AF647		SLA-(Enc) OVA-AF647			SLA-(Adm) OVA-AF647		
		Mean	SEM	Mean	SEM	Mean	SEM	P Value	Mean	SEM	P Value
1	Total Live Cells	70,880	16,026	82,840	7,901	250,000	55,571	.0082	142,200	22,936	.5532
	Neutrophils	4,861	1,454	7,292	1,146	39,223	6,515	.0222	53,430	12,009	.0012
	Monocytes	10,599	2,491	10,696	1,346	26,007	6,311	.0353	13,339	1,698	.9518
	Macrophages	11,209	2,719	15,628	1,183	64,249	13,745	.0021	27,598	6,565	.6999
	DCs	9,868	2,826	9,650	968	41,463	9,428	.0020	13,640	1,908	.9424
	B cells	12,992	4,323	10,869	2,181	7,200	3,027	.8082	6,753	1,054	.7502
	CD8 ⁺ T cells	8,256	2,013	10,144	1,614	26,975	7,387	.0371	9,329	1,053	.9988
3	Total Live Cells	56,575	6,917	84,160	10,636	182,980	51,886	.5891	481,800	91,409	.0006
	Neutrophils	1,092	111	2,140	667	16,989	6,021	.4958	71,239	12,763	<.0001
	Monocytes	6,213	811	9,325	1,551	20,725	6,605	.6036	42,225	10,407	.0120
	Macrophages	11,089	2,455	24,734	4,205	55,410	14,383	.6449	154,855	32,059	.0008
	DCs	17,614	7,427	27,220	4,974	46,629	15,116	.5957	65,470	12,365	.1007
	B cells	5,473	1,887	3,807	926	3,311	566	.9819	2,901	157	.9034
	CD8 ⁺ T cells	4,578	1,646	3,511	1,003	6,714	1,686	.9890	67,958	13,829	<.0001

C57BL/6 mice were injected i.m. into the left TA muscle with 20 μ g OVA-AF647, SLA-(Adm) OVA-AF647 or SLA-(Enc) OVA-AF647. At days 1 and 3 post-injection, the left TA muscles were collected and processed for total live cell counting through the Cellometer and flow cytometric analysis of immune cell types. N = 4–5 mice per group. Statistical significance was analyzed by one-way ANOVA followed by Tukey's multiple comparisons test. *P* values indicate comparison of immune cell numbers relative to the OVA-AF647 group, where $p < .05$ is considered statistically significant.

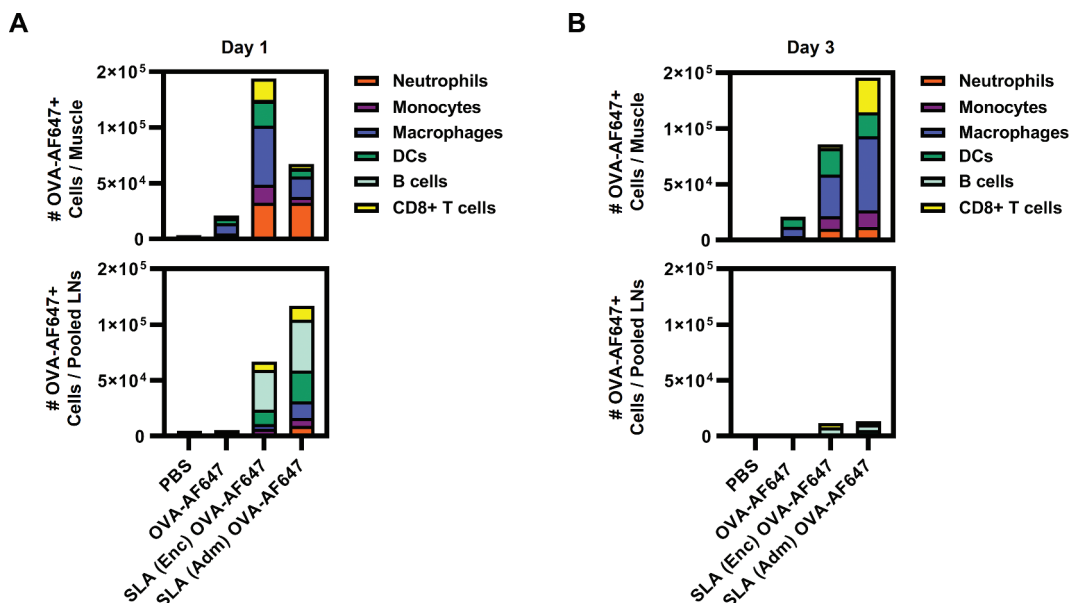


Figure 1. Immune cell recruitment and OVA-AF647 antigen uptake in mice treated with SLA (Enc) and (Adm). C57BL/6 mice were injected i.m. into the left TA muscle with AF647-labeled OVA, AF647-labeled OVA encapsulated in SLA (SLA (Enc) OVA-AF647), AF647-labeled OVA admixed with SLA (SLA (Adm) OVA-AF647). At days 1 and 3 post-injection, the left TA muscle and draining LNs (pooled inguinal and popliteal) were collected and processed for subsequent live cell counting and flow cytometric analysis. (A) OVA-AF647⁺ immune cell numbers in TA muscles and pooled LNs at day 1 post-injection. (B) OVA-AF647⁺ immune cell numbers in TA muscles and pooled LNs at day 3 post-injection. Data are presented as stacked means of OVA-AF647⁺ immune cell types. N = 5 mice per group.

Table 2. Numbers of immune cell types in pooled draining LNs of mice injected i.m. with SLA (Enc) and (Adm).

Time Point (Day)	Immune Cell Type	PBS		OVA-AF647		SLA-(Enc) OVA-AF647			SLA-(Adm) OVA-AF647		
		Mean	SEM	Mean	SEM	Mean	SEM	P Value	Mean	SEM	P Value
1	Total Live Cells	2,152,000	337,867	2,328,200	973,103	6,094,000	1,364,367	.1423	10,564,000	1,578,748	.0007
	Neutrophils	1,467	245	1,022	346	18,212	12,373	.2969	24,933	4,859	.0907
	Monocytes	484,331	76,041	535,033	228,679	1,274,051	262,863	.3670	2,932,929	511,126	.0003
	Macrophages	6,036	1,583	8,393	4,097	40,871	18,132	.1380	63,656	6,958	.0060
	DCs	77,043	15,255	55,479	23,371	188,245	66,900	.1049	193,783	23,635	.0871
	B cells	427,248	87,533	550,174	219,507	1,728,380	407,434	.1019	2,517,008	479,657	.0039
	CD8 ⁺ T cells	629,662	80,509	672,897	285,429	1,661,842	370,783	.1664	2,888,313	424,203	.0008
3	Total Live Cells	2,395,000	380,909	2,144,000	626,567	4,894,000	1,198,564	.3544	8,678,000	1,718,076	.0051
	Neutrophils	868	247	708	156	1,825	967	.9430	6,682	2,555	.0414
	Monocytes	573,391	92,474	520,775	148,433	1,195,859	271,253	.4144	2,271,098	488,146	.0045
	Macrophages	5,737	1,005	7,263	2,028	25,260	7,730	.3043	56,183	10,941	.0009
	DCs	43,519	13,368	37,023	10,866	94,285	22,078	.2597	167,620	30,788	.0027
	B cells	417,592	19,357	389,336	134,942	842,974	283,304	.5369	1,916,714	327,913	.0017
	CD8 ⁺ T cells	798,911	170,986	704,505	200,780	1,665,906	396,697	.3249	2,571,289	581,472	.0172

C57BL/6 mice were injected i.m. into the left TA muscle with 20 µg OVA-AF647, SLA-(Adm) OVA-AF647 or SLA-(Enc) OVA-AF647. At days 1 and 3 post-injection, the left draining LNs (pooled inguinal and popliteal) were collected and processed for total live cell counting through the Cellometer and flow cytometric analysis of immune cell types. N = 4–5 mice per group. Statistical significance was analyzed by one-way ANOVA followed by Tukey's multiple comparisons test. P values indicate comparison of immune cell numbers relative to the OVA-AF647 group, where $p < .05$ is considered statistically significant.

injection was measured at various time-points following injection of CF770-labeled OVA alone, or formulated with SLA (Enc or Adm) (representative images shown in Figure 2A). With both SLA formulations, the labeled OVA is more strongly retained at the injection site for at least 24 h when compared to OVA alone (Figure 2B). The fluorescence intensity appears to be maintained for a longer period of time *in vivo* at the injection site at 48 h in mice that received SLA (Enc) OVA-CF770 compared to CF770-labeled OVA alone or SLA (Adm) OVA-CF770. However, this difference was not apparent at later time points (72 h, 96 h and 168 h). Overall, both tested SLA formulations appear to increase the retention of the antigen at the injection site, but the SLA (Enc) formulation is able to maintain it for slightly longer (i.e. 48 h) (Figure 2B).

SLA (Enc) and (Adm) formulations induce early local cytokine responses *in vivo*

The impact of the two SLA archaeosome formulations on cytokine/chemokine induction in the injected muscle was measured following immunization with OVA-AF647 alone or formulated with SLA (Enc) or (Adm). The same formulations used for the antigen uptake study above were used for this analysis. The levels of multiple cytokines and chemokines (i.e., G-CSF, GM-CSF, IL-6, KC, MCP-1 and MIP-2) appear higher in the muscles of mice injected with either SLA-adjuvanted formulation when compared to antigen alone or PBS controls (Table 3). For example, levels of KC were ~2-6 fold higher in the muscles immunized with the SLA-adjuvanted formulations as compared to antigen alone (mean ± SEM; 100.3 ± 15.4, 211.7 ± 105.1 and

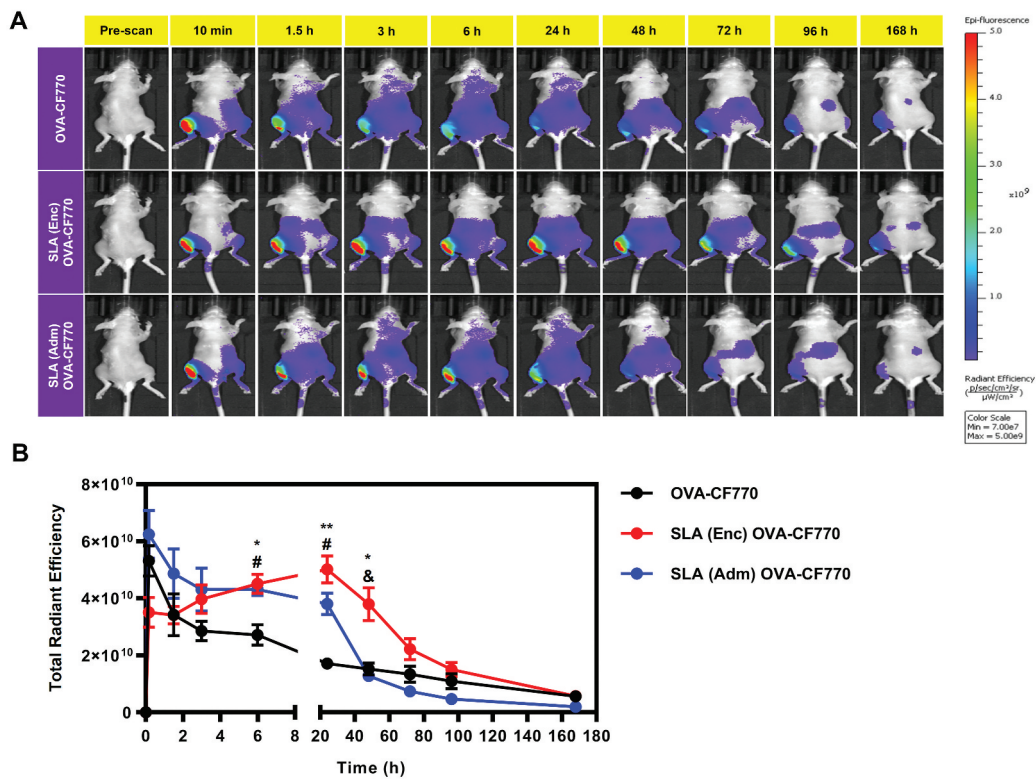


Figure 2. *In Vivo* Biodistribution of OVA-CF770 following immunization with formulations adjuvanted with SLA (Enc) and (Adm). C57BL/6 albino mice were injected i.m. with CF770-labeled ovalbumin alone (OVA-CF770, 20 μ g), CF770-labeled OVA encapsulated in SLA (SLA (Enc) OVA-CF770), or CF770-labeled OVA admixed with SLA (SLA (Adm) OVA-CF770). Whole-body imaging was conducted to localize CF770-labeled OVA at various time points. (A) A representative image series of a single mouse per group imaged at the time points indicated is shown. (B) The total fluorescent signals *in vivo* obtained from an ROI of the injection site were quantified and presented as a line graph relating total radiant efficiency (i.e. total fluorescence) over time (group means \pm SEM). N = 4 mice per group. Statistical significance was analyzed by two-way ANOVA followed by Tukey's multiple comparisons test. *, # or &: $p < .05$, **: $p < .01$. * and ** indicate comparison between SLA Enc and OVA-CF770. # indicates comparison between SLA Adm and OVA-CF770. & indicates comparison between SLA (Enc) and SLA (Adm).

Table 3. Cytokine and chemokine levels in the injection site after treatment with SLA (Enc) and (Adm).

Cytokine/Chemokine	PBS		OVA-AF647		SLA-(Enc) OVA-AF647			SLA-(Adm) OVA-AF647		
	Mean	SEM	Mean	SEM	Mean	SEM	P Value	Mean	SEM	P Value
G-CSF	1.55	0.2	49.73	4.58	139.3	40.64	.0246	117.9	13.18	.1054
GM-CSF	1.5	0.18	1.9	0.29	4.2	1.6	.5794	18	2	<.0001
IL-6	7.8	0.5	32	6.5	96	23	.8919	466	120	.0004
KC	19.77	2.59	100.3	15.40	211.7	105.1	.5988	660.1	76.78	<.0001
MCP-1	128.3	18.21	250.3	52.43	637.0	164.0	.1487	1706	195.5	<.0001
MIP-2	11.36	1.43	58.78	9.46	220.9	100.3	.1833	333.3	59.87	.0115

C57BL/6 mice were injected i.m. into the left TA muscle with OVA-AF647, SLA-(Adm) OVA-AF647 or SLA (Adm) OVA-AF647. The left TA muscles were collected and processed at 6 h post-injection for the measurement of cytokine and chemokine expression levels (pg/mg of total protein). N = 3–5 mice per group. Statistical significance was analyzed by one-way ANOVA followed by Tukey's multiple comparisons test. P values indicate comparison of cytokine/chemokine levels relative to the OVA-AF647 group, where $p < .05$ is considered statistically significant.

660.1 \pm 76.78 for OVA-AF647 alone, SLA (Enc) and SLA (Adm) formulations, respectively). A similar trend was observed with MIP-2 (mean \pm SEM; 58.78 \pm 9.46, 220.9 \pm 100.3 and 333.3 \pm 59.87 for OVA-AF647 alone, SLA (Enc) and SLA (Adm) formulations, respectively). These results indicate that archaeosome formulations (Enc or Adm) can induce early cytokine/chemokine induction at the vaccination site.

Macrophages phagocytose SLA formulations more efficiently compared to DCs

As APCs play a key role in the induction of immune responses *in vivo*, we sought to more directly evaluate the impact of the

different SLA formulation on their activation *in vitro*. Firstly, we measured the ability of antigen-presenting cells, namely DCs and macrophages, to phagocytose SLA archaeosomes. SLA (Enc) and (Adm) formulations were stained with the phospholipid rhodamine DHPE labeled with red-fluorescent fluorophore prior to incubation with BMDMs and BMDCs *in vitro* and uptake measured using the InCyte[®] S3 system. While BMDMs exhibited a linear increase in total integrated red intensity up to 6 h with both archaeosome formulations (Figure 3), only baseline levels were detected in DCs (Figure 3) suggesting that macrophages were more capable of phagocytosing SLA archaeosomes. Treatment of macrophages with cytoD, an inhibitor of F-actin polymerization and phagocytic

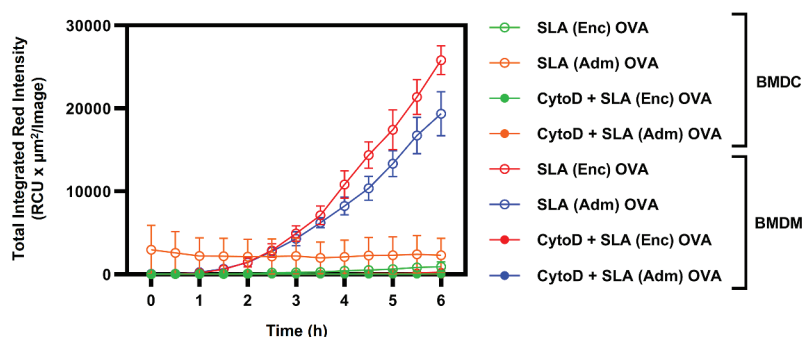


Figure 3. Kinetics of SLA (Enc) and (Adm) uptake by BMDMs and BMDCs *in vitro*. BMDMs and BMDCs were seeded in duplicate at 1×10^4 cells per well. Data shown are from one representative experiment of two independent experiments. Cells were incubated with SLA (Enc or Adm OVA) stained with rhodamine DHPE labeled with red-fluorescent fluorophore. Cellular uptake of SLA was quantified over time by measuring the total integrated red intensity (RCU $\times \mu\text{m}^2/\text{image}$) per well. Cells pre-incubated with cytoD served as phagocytosis negative controls. Data are presented as mean \pm SEM.

cup formation, resulted in a drastic reduction in total integrated red intensity confirming that the uptake of SLA by the cells was mediated through phagocytosis (Figure 3 and Supplemental Figure 1).²¹

Stimulation of macrophages and DCs by SLA formulations promotes distinct cytokine expression profiles *in vitro*

To further evaluate the ability of SLA to activate APCs *in vitro*, we measured the expression of pro-inflammatory cytokines and chemokines by BMDMs and BMDCs when stimulated with OVA, SLA, SLA (Enc) OVA or SLA (Adm) OVA. Both SLA (Enc) and (Adm) formulations resulted in increased cytokine production by BMDMs. Overall, the SLA (Enc) formulation induced significantly higher levels of TNF- α , MIP-1 α and MIP-1 β compared to OVA and SLA alone (Figure 4). Meanwhile, the SLA (Adm) formulation induced a significant increase in MIP-1 α and MIP-1 β to similar levels as SLA alone. In contrast, there was no significant increase in cytokine and chemokine levels produced by BMDCs when stimulated with any of the formulations at 24 h post-pulsing (data not shown). These results indicate the increased sensitivity of BMDMs to SLA-mediated immune activation relative to BMDCs *in vitro*.

Antigen-pulsed macrophages and DCs induce distinct CD8⁺ T cell activation profiles *in vitro*

We next evaluated the ability of BMDCs or BMDMs pre-exposed to OVA alone or formulated within different archaeosome formulations to directly activate OVA-specific CD8⁺ T cells. Our activation targets were splenic cells from transgenic OT-1 mice that have CD8⁺ T cells that specifically express MHC class I-restricted OVA-specific T cell receptors.²² The activation of OT-1 CD8⁺ T cells at 24 h post-co-culture was determined through flow cytometric analysis of cell-surface CD44 and CD69 and intracellular IFN- γ expression (representative plots shown in Figure 5A). BMDMs pulsed with OVA alone gave a significant increase in CD44⁺CD69⁺ CD8⁺ T cell percentages, which were not further increased if OVA was formulated with either SLA (Enc) or (Adm) (Figure 5B). In fact, it appeared that the SLA (Adm) formulation had a negative impact on the ability of macrophages to activate the OVA-specific CD8 T cells. While DCs pulsed with OVA alone showed only a modest increase in CD44⁺CD69⁺ CD8⁺ T cell percentages relative to unstimulated DCs (Figure 5B), the percentages of both CD44⁺CD69⁺ and IFN- γ ⁺ CD8⁺ T cells were significantly increased in DCs pulsed with SLA (Enc) but not with the SLA (Adm) formulation.

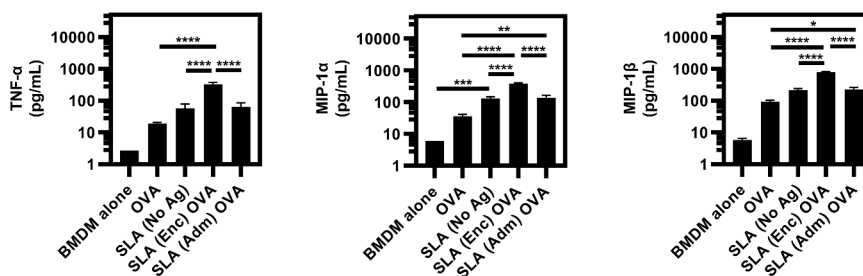


Figure 4. Cytokine and chemokine expression by BMDMs upon *in vitro* stimulation with SLA (Enc) and (Adm) vaccine formulations. BMDMs were pulsed in duplicate wells with OVA alone, SLA alone, SLA (Enc) OVA or SLA (Adm) OVA. Cytokine and chemokine levels in cell culture supernatants were measured at 24 h post-pulsing. Data are pooled from two independent experiments. (A) TNF- α , MIP-1 α and MIP-1 β levels (pg/mL) in antigen-pulsed BMDM culture supernatants are shown. Data are presented as mean \pm SEM. Statistical significance was analyzed by one-way ANOVA followed by Tukey's multiple comparisons test. *: $p < .05$, **: $p < .01$, ***: $p < .001$, ****: $p < .0001$.

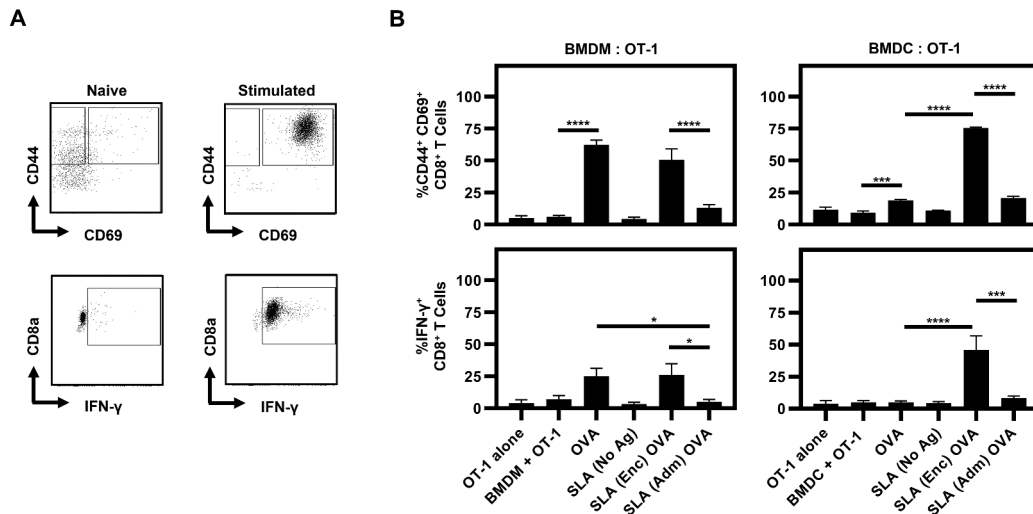


Figure 5. CD8⁺ T cell activation induced by BMDCs and BMDMs pulsed with SLA (Enc) and (Adm) vaccine formulations *in vitro*. BMDMs and BMDCs were co-cultured with OT-1 cells in duplicate wells at 1:1 cell ratio 24 h after pulsing with SLA alone, OVA alone, SLA (Enc) OVA or SLA (Adm) OVA. Data are pooled from four independent experiments. (A) Representative flow cytometry plots showing CD44, CD69 and IFN-γ expression by naïve and stimulated OT-1 CD8⁺ T cells. (B) Percentages of CD44⁺CD69⁺ and IFN-γ⁺ CD8⁺ T cells in BMDC:OT-1 and BMDM:OT-1 co-cultures at 24 h post-co-culture. Data are presented as mean ± SEM. Statistical significance was analyzed by one-way ANOVA followed by Tukey's multiple comparisons test. *: $p < .05$, ***: $p < .001$, ****: $p < .0001$.

OVA adjuvanted with SLA (Enc) or SLA (Adm) formulations enhances mouse survival against B16-OVA challenge

To determine whether the differences noted above mainly in the *in vitro* T cell activation system would translate *in vivo* with regards to vaccine efficacy, mice were first immunized with either OVA alone or with SLA (Enc) and (Adm) formulations. Mice were then challenged with 5×10^5 B16-OVA melanoma tumor cells at 3 weeks post-immunization. As expected, mice that received OVA alone exhibited similarly low percent survival and rapid increase in tumor volumes as naïve mice, with both groups having a median survival of 21 days (Figure 6 and Supplemental Figure 2). In contrast, median survival was significantly increased upon treatment with OVA in combination with SLA to 41 and 60 days with SLA (Enc) and (Adm) formulations, respectively. These increased survival rates correlated with delayed tumor growth compared to the OVA and naïve groups. Overall, our results

indicate that SLA archaeosomes enhance vaccine-induced tumor protection *in vivo* when simply admixed with antigen or used to encapsulate antigen.

Discussion

Archaeosomes are prime adjuvant candidates due to their strong immunostimulatory properties, effective induction of humoral and cell-mediated immunity to numerous antigens and robust ability to confer protective immunity in multiple models of murine infection and cancer.^{3,5-11} Our novel SLA-based archaeosomes retain the robust adjuvant properties of traditional TPL formulations when antigen is encapsulated, while gaining the key advantage of a simplified semi-synthetic single lipid formulation. Recently, we showed that admixing antigen with SLA offers increased consistency of antigen-to-lipid ratios and no antigen loss during formulation

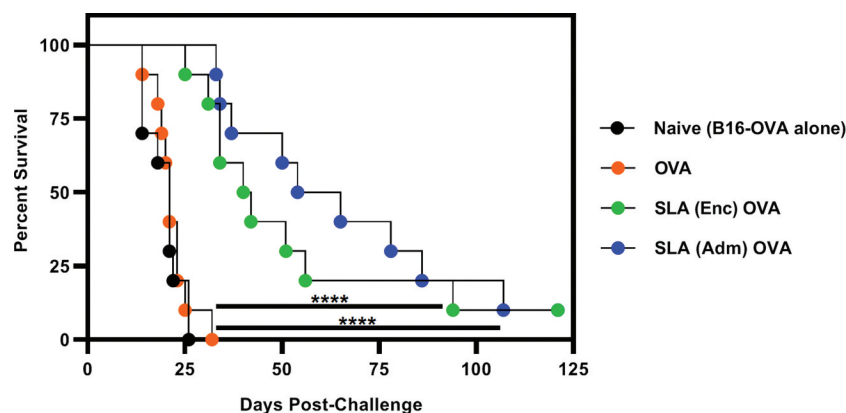


Figure 6. Survival of mice treated with a single dose of SLA (Enc) or (Adm) vaccine formulations and challenged with B16-OVA melanoma tumor cells. C57BL/6 mice were immunized by i.m. injection into the left TA muscle with SLA (Adm) OVA, SLA (Enc) OVA, or OVA alone. At 3 weeks post-injection, mice were injected s.c. with 5×10^5 B16-OVA tumor cells in the mid-dorsal flank. Mouse deaths were recorded upon reaching the humane and experimental endpoints. N = 10 mice per group. Survival curves were analyzed using the Gehan-Breslow-Wilcoxon test. ****: $p < .0001$.

relative to antigen encapsulation, with no negative effect on the quality of antigen-specific responses.⁷ However, the consequences of the mode of antigen delivery (incorporated within or outside of the liposome structure) on the activation of early innate immune responses, particularly immune cell recruitment, antigen uptake and pro-inflammatory cytokine expression have not been evaluated. The relative contributions of APCs, particularly DCs and macrophages toward the induction of antigen-specific T cell immunity with these vaccine formulations are also not understood. Therefore, this study was performed to further gain insight into SLA-induced innate immune mechanisms that shape the development of protective immunity.

Immune cell infiltration and activation are among the key early events in the local innate immune response after vaccination. Antigen is encountered by APCs and presented to cytotoxic CD8⁺ and helper CD4⁺ T cells, which can lead to T cell activation if sufficient APC co-stimulation is received.^{1,23} Cytokine expression by CD4⁺ T cells also supports the functions of mononuclear phagocytes and antibody production by B cells.²³ Thus, enhancing immune cell infiltration with optimal adjuvant-antigen combinations can theoretically increase APC exposure to antigen and improve the magnitude of subsequent adaptive responses.

SLA (Adm) and (Enc) appeared to preferentially promote immune cell recruitment and OVA uptake in the draining LNs and muscle, respectively, at day 1 post-treatment. Furthermore, the increase in immune cell recruitment and OVA uptake in the muscle was more pronounced at day 3 post-treatment with SLA (Adm). These differences in immune cell and antigen distribution between the SLA formulations may be attributed to the rapid cellular uptake and/or diffusion of soluble antigens to draining LNs with SLA (Adm), in contrast to increased antigen retention in the injection site with SLA (Enc). Consistent with these observations, our *in vivo* biodistribution results showed increased retention of OVA at the injection site with both SLA (Enc) and SLA (Adm) formulations relative to OVA alone for up to 24 h. However, SLA (Enc) was able to maintain higher amounts of OVA at the injection site for a further 24 h (i.e. 48 h post-administration), while SLA (Adm) was not. Taken together, these results indicate that OVA encapsulation within archaeosomes may promote a more sustained release of antigen in the injection site (depot effect), that could potentially alter the kinetics of antigen uptake/trafficking when compared to the admixed formulation.²

We previously showed that in the absence of antigen, SLA-based archaeosomes induced mild necrosis of muscle tissue that was self-resolving at a 1 mg dose.³ This is another factor that can influence immune cell recruitment and immune activation. The widely used aluminum-based adjuvant (alum) has been shown to induce immunostimulatory activity by triggering cell death and the subsequent release of host cell DNA at the injection site.²⁴ Extracellular host DNA can act as damage-associated molecular patterns (DAMPs), which can activate the immune system through various pattern recognition receptor (PRR) signaling pathways.^{24,25} Whether SLA-based archaeosomes require immunogenic cell death for their adjuvant activity would need to be confirmed in future studies.

Batch-to-batch differences in SLA (Enc) antigen-to-lipid ratios are attributed to varying antigen entrapment efficiencies.^{7,16,17} We show that SLA (Enc) and (Adm) induce cytokine/chemokine expression in the injected muscle. The increased lipid content in the SLA (Adm) formulation (1000 vs. 238 µg with SLA (Enc)) could explain the increased level of cytokines such as IL-6 seen with SLA (Adm). Thus, increasing lipid content in SLA may enhance adjuvant-induced cytokine responses, consistent with other model lipid adjuvants such as Glucopyranosyl Lipid A (GLA) and synthetic Monophosphoryl Lipid A (PHAD[®]).^{26,27} Lipid A, which is the conserved molecular pattern of lipopolysaccharide (LPS), interacts with the heterodimer complex comprised Toll-like receptor 4 (TLR4) and myeloid differentiation factor 2 (MD-2) toward the induction of pro-inflammatory responses.²⁸ The precise mechanism of ligand-receptor engagement and immune activation by SLA is yet to be confirmed. Taken together, our results indicate that both SLA (Adm) and (Enc) enhance immune cell infiltration, antigen uptake and retention. However, the nature of the SLA archaeosome formulation (i.e., encapsulated or admixed) and the adjuvant lipid content may lead to some differences in the rate of antigen retention at the injection site, immune cell infiltration and cytokine induction. Despite any differences observed in these parameters, both SLA formulations induce strong adaptive antigen-specific immune responses as demonstrated in this study and in our previous work.

Phagocytic immune cells such as macrophages and DCs are natural targets of liposomes for intracellular drug and therapy delivery. We previously showed archaeosomes with TPLs derived from *Methanospirillum hungatei* were phagocytosed by murine J774A.1 monocyte-macrophages with greater efficiency compared to conventional liposomes composed of ester lipids dipalmitoylphosphatidylcholine (DPPC) or dimyristoylphosphatidylcholine (DMPC):dimyristoylphosphatidylcholine (DMPG):cholesterol.²⁹ Uptake of MS archaeosomes by murine peritoneal macrophages and BMDCs was also shown to occur via PS receptor recognition of phosphoserine head groups on the archaeosome surface.^{18,19} In the current study, we demonstrate the increased efficiency of BMDCs in phagocytic uptake of SLA (Enc) and (Adm) formulations when compared to BMDCs. These results also indicate that BMDC uptake of SLA is not differentially modulated by the presence of the antigen within or outside the archaeosome in the SLA (Enc) and SLA (Adm) formulations, respectively. As professional APCs, macrophages and DCs play the critical role of inducing antigen-specific T cell responses through the presentation of antigen-derived peptides to CD8⁺ and CD4⁺ T cells via major histocompatibility complex (MHC) class I and II molecules, respectively.^{30,31} While macrophages and DCs share key features, their phagocytic functions produce different outcomes. Macrophages exhibit high lysosomal proteolytic activity against internalized pathogens within phagosomal compartments as a mechanism of host defense.³² In contrast, DCs exhibit reduced phagosomal degradation relative to macrophages due to less efficient recruitment of lysosomal proteases to phagosomes.³²⁻³⁴ This partial degradation of internalized antigen better enables DCs to preserve antigenic peptides for presentation to T cells.³²

In the current study, we aimed to gain insight into the early innate immune responses generated by BMDMs and BMDCs toward the induction of antigen-specific T cells. Increased phagocytic uptake of SLA (Enc) and (Adm) formulations by BMDMs correlated with a general increase in cytokine/chemokine induction compared to BMDCs. SLA (Adm)-treated BMDMs also showed similarly high expression levels of cytokines/chemokines in the presence or absence of antigen, indicating that cytokine/chemokine induction is primarily mediated by SLA. While traditional TPL archaeosome formulations were taken up by BMDCs in addition to macrophages, SLA-based formulations appear to target and activate BMDMs more readily. This indicates that the uptake (and subsequent cytokine signaling) of TPL archaeosomes such as MS by BMDCs was primarily dependent on the phosphoserine-PS receptor engagement, which is not possible with SLA formulations due to their lack of any PS domains. Traditional archaeosomes also inherently exhibit a diverse composition of lipids and carbohydrate moieties, which could ultimately impact adjuvant uptake and subsequent induction of immune responses.⁵ Thus, BMDMs are suitable targets for SLA in the induction of early innate immune response *in vitro*.

Naïve CD8⁺ T cells undergo initial activation (priming) upon interaction with APCs presenting peptide/MHC complexes.³⁵ Activated CD8⁺ T cells upregulate various cell-surface markers, including CD44 and CD69, as well as pro-inflammatory cytokines such as IFN- γ .^{36,37} Despite having lower overall phagocytic efficiency relative to BMDMs, SLA (Enc)-treated BMDCs enhanced antigen-specific expression of CD44, CD69 and IFN- γ by CD8⁺ T cells at 24 h post-co-culture with OT-1 splenocytes compared to OVA alone or SLA (Adm)-OVA-treated BMDCs (Figure 5B). These results indicate that antigen delivery rather than the magnitude of SLA uptake is critical in BMDC-induced antigen-specific T cell responses *in vitro*. In contrast, CD44⁺CD69⁺ CD8⁺ T cell percentages were increased by OVA alone or SLA (Enc)-OVA post-co-culture with BMDMs. We did not observe a significant increase in T cell activation induced by BMDMs pulsed with SLA-(Adm) OVA (Figure 5B). This may be attributed to increased competition for uptake between OVA and SLA by a fixed number of BMDMs, which would not occur with the SLA (Enc) formulation as the uptake of antigen and adjuvant would occur simultaneously due to their colocalization within the same particle. In addition, SLA (Enc) may induce enhanced antigen-specific responses *in vitro* by providing a more uniform adjuvant-antigen distribution to a fixed number of BMDCs relative to the SLA (Adm) formulations. In addition, as antigen processing and presentation of antigen epitopes are also required to activate CD8⁺ T cells, it may be possible that the SLA (Adm) formulation is less able than SLA (Enc) to mediate this process on purified cell populations *in vitro*. This does not appear to be an issue *in vivo* as SLA (Adm) and SLA (Enc) formulations have been shown to induce similar levels of antigen-specific CD8 + T cells following immunization.

There are limitations to the conclusions that can be drawn from *in vitro* immune systems, as they cannot completely reproduce the immune system's complexity *in vivo*, in particular the immune cell infiltration/trafficking that would occur

following immunization. Despite the observed differences in antigen processing *in vitro*, the robust immune cell infiltration induced by SLA (Enc) and (Adm) formulations, and consequently increased exposure of APCs to antigen, appears to be sufficient to promote similarly enhanced antigen-specific responses *in vivo*. Whether the mode of antigen delivery will considerably impact individuals with innate immune-altered conditions, including age-associated immune dysregulation and DC defects in primary immunodeficiency disorders are yet to be determined.^{38,39} However, studies conducted in aged mice (~2 years old) with influenza HA antigen demonstrated that the SLA (Adm)-HA formulation was as efficacious as SLA (Enc)-HA in protecting mice from viral challenge.¹⁰ Furthermore, the relative contributions of DC subsets other than BMDCs on SLA-mediated innate immune activation and induction of antigen-specific responses would need to be confirmed in future studies. Lymphoid tissue CD8⁺ DCs and non-lymphoid tissue CD103⁺ DCs specialize in cross-presentation, wherein exogenous antigens are presented to CD8⁺ T cells via MHC class I.⁴⁰ Thus, it is possible that these DC subsets contribute to presentation of antigens in SLA (Adm) formulations *in vivo*.

Developing immunity to cancer is an ongoing challenge due to the poor immunogenicity of most tumors and immune-suppressive mechanisms within the tumor microenvironment. Accordingly, the identification of T cell-recognized tumor antigens, as well as optimization of vaccination regimens remain critical strategies toward the development of novel cancer therapies that rely on antigen-specific anti-tumor responses. Antigen entrapment in archaeosome vesicles was initially thought to enhance MHC class I processing required for induction of CD8⁺ T cell responses through direct delivery of antigen into the cytosol. Mice immunized with ovalbumin (OVA) antigen entrapped in MS liposomes (MS-OVA) exhibit delayed susceptibility to B16 melanoma tumors expressing OVA (B16-OVA).⁹ This was associated with increased OVA-specific CD8⁺ T cell responses compared to mice immunized with OVA alone. Tumor protection was further enhanced in combination with anti-PD-1, anti-PD-L1 and anti-CTLA-4 checkpoint inhibitor immunotherapies.⁹ However, we have previously shown with our prime-boost vaccination strategy using a simplified SLA (Adm) formulation that exogenous antigens are similarly capable of inducing robust antigen-specific humoral/cell-mediated responses and tumor immunity as SLA (Enc) *in vivo*.^{7,11} We show in the current study that even a single immunization with SLA (Adm) and (Enc) formulations with normalized lipid content (1,000 μ g) can confer similar enhanced protection from B16-OVA melanoma tumor challenge. Whether the similarly enhanced protection conferred by SLA (Adm) and its SLA (Enc) counterpart can be partially attributed to cross-presentation by other specialized DC subsets *in vivo* remains to be elucidated.

There are some limitations to the current study. Most importantly, the results of studies conducted using mice, while important to provide preliminary data on safety, efficacy and potential mechanism of action may not necessarily predict the findings in larger species, in particular humans. Furthermore, *in vitro* studies may not necessarily predict *in vivo* results given the complexities of an intact immune

system. It would also have been beneficial to include a full dose-response of lipid in both formulations, although this was out-of-scope of the current study, as additional dose-related effects may have become apparent.

In summary, we demonstrate the roles of SLA archaeosomes in the induction of innate immunity and development of antigen-specific responses using *in vivo* and *in vitro* models. While some differences were observed in the antigen retention and uptake rates at the injection site between the SLA (Enc) and SLA (Adm) formulations, both formulations generate a strong increase in immunostimulatory activity, leading to enhanced protective immunity against tumor challenge. Future studies characterizing ligand-receptor engagement and cell signaling will also help improve our understanding of the mechanism of action of SLA and identify new targets toward the development of effective vaccine strategies.

Abbreviations

adm	admixed
BM	bone marrow
BMDM	bone marrow-derived macrophage
BMDC	bone marrow-derived dendritic cell
cytoD	cytochalasin D
DC	dendritic cell
enc	encapsulated
i.m.	intramuscular
PS	phosphatidylserine
s.c.	subcutaneous
SLA	sulfated lactosylarchaeol (6'-sulfate- β -D-Galp-(1,4)- β -D-Glcp-(1,1)-archaeol)

Acknowledgments

The authors would like to acknowledge Renu Dudani for assistance with cell counting and tissue processing. We thank Scott McComb, Mohammad P. Jamshidi, Janelle Sauvageau and Dean Williams for providing scientific advice. We would also like to thank Shawn Makinen, Mario Mercier, Becky Wilson and Abbey Robertson for performing the i.m. injections and the NRC Animal Resources group for monitoring the health status of the study mice.

Author contributions

GA, YJ, BA and MJM conceptualized the study and designed experiments. GA, VC and UI performed the experiments. YJ, VC, LD, EL, UDH and SR prepared the vaccines. GA, YJ, BA, VC and MJM analyzed the data. FCS performed the tumor s.c. injections and contributed to the discussion of ideas. GA, YJ, BA, UI and MJM wrote the manuscript. All authors contributed to the discussions, provided critical feedback and edited the manuscript.

Disclosure of potential conflicts of interest

Lakshmi Krishnan is an inventor on various archaeosome patents and patent applications. All other authors declare no conflict of interest, nor competing financial interests.

Disclosure of potential conflicts of interest

No potential conflicts of interest were disclosed.

ORCID

Michael J. McCluskie  <http://orcid.org/0000-0001-5538-1363>

References

- Liang F, Lore K. Local innate immune responses in the vaccine adjuvant-injected muscle. *Clin Transl Immunol.* 2016;5:e74. doi:10.1038/cti.2016.19.
- Awate S, Babiuk LA, Mutwiri G. Mechanisms of action of adjuvants. *Front Immunol.* 2013;4:114. doi:10.3389/fimmu.2013.00114.
- Akache B, Stark FC, Iqbal U, Chen W, Jia Y, Krishnan L, McCluskie MJ. Safety and biodistribution of sulfated archaeal glycolipid archaeosomes as vaccine adjuvants. *Hum Vaccin Immunother.* 2018;14:1746–59. doi:10.1080/21645515.2017.1423154.
- Tandrup SS, Foged C, Korsholm KS, Rades T, Christensen D. Liposome-based adjuvants for subunit vaccines: formulation strategies for subunit antigens and immunostimulators. *Pharmaceutics.* 2016;8(1):7. doi:10.3390/pharmaceutics8010007
- Haq K, Jia Y, Krishnan L. Archaeal lipid vaccine adjuvants for induction of cell-mediated immunity. *Expert Rev Vaccines.* 2016;15:1557–66. doi:10.1080/14760584.2016.1195265.
- Akache B, Stark FC, Jia Y, Deschatelets L, Dudani R, Harrison BA, Agbayani G, Williams D, Jamshidi MP, Krishnan L, et al. Sulfated archaeol glycolipids: comparison with other immunological adjuvants in mice. *PLOS ONE.* 2018;13(12):e0208067. doi:10.1371/journal.pone.0208067.
- Jia Y, Akache B, Deschatelets L, Qian H, Dudani R, Harrison BA, Stark FC, Chandan V, Jamshidi MP, Krishnan L, et al. A comparison of the immune responses induced by antigens in three different archaeosome-based vaccine formulations. *Int J Pharm.* 2019;561:187–96. doi:10.1016/j.ijpharm.2019.02.041.
- McCluskie MJ, Deschatelets L, Krishnan L. Sulfated archaeal glycolipid archaeosomes as a safe and effective vaccine adjuvant for induction of cell-mediated immunity. *Hum Vaccine Immunother.* 2017;13:2772–79. doi:10.1080/21645515.2017.1316912.
- Stark FC, Weeratna RD, Deschatelets L, Gurnani K, Dudani R, McCluskie MJ, Krishnan L. An archaeosome-adjuvanted vaccine and checkpoint inhibitor therapy combination significantly enhances protection from murine melanoma. *Vaccines (Basel).* 2017;5:38.
- Stark FC, Akache B, Ponce A, Dudani R, Deschatelets L, Jia Y, Sauvageau J, Williams D, Jamshidi MP, Agbayani G, et al. Archaeal glycolipid adjuvanted vaccines induce strong influenza-specific immune responses through direct immunization in young and aged mice or through passive maternal immunization. *Vaccine.* 2019;37:7108–16. doi:10.1016/j.vaccine.2019.07.010.
- Stark FC, Agbayani G, Sandhu JK, Akache B, McPherson C, Deschatelets L, Dudani R, Hewitt M, Jia Y, Krishnan L, et al. Simplified admix archaeal glycolipid adjuvanted vaccine and checkpoint inhibitor therapy combination enhances protection from murine melanoma. *Biomedicines.* 2019;7(4):91. doi:10.3390/biomedicines7040091.
- Conlan JW, Krishnan L, Willick GE, Patel GB, Sprott GD. Immunization of mice with lipopeptide antigens encapsulated in novel liposomes prepared from the polar lipids of various Archaeobacteria elicits rapid and prolonged specific protective immunity against infection with the facultative intracellular pathogen, *Listeria monocytogenes*. *Vaccine.* 2001;19:3509–17. doi:10.1016/s0264-410x(01)00041-x.
- Krishnan L, Deschatelets L, Stark FC, Gurnani K, Sprott GD. Archaeosome adjuvant overcomes tolerance to tumor-associated melanoma antigens inducing protective CD8 T cell responses. *Clin Dev Immunol.* 2010;2010:578432. doi:10.1155/2010/578432.

14. Landi A, Law J, Hockman D, Logan M, Crawford K, Chen C, Kundu J, Ebensen T, Guzman CA, Deschatelets L, et al. Superior immunogenicity of HCV envelope glycoproteins when adjuvanted with cyclic-di-AMP, a STING activator or archaeosomes. *Vaccine*. 2017;35:6949–56. doi:10.1016/j.vaccine.2017.10.072.
15. Akache B, Deschatelets L, Harrison BA, Bhat RA, Nazir QU, Haq AU, Malik HU, Fazilli MUR, Gopalakrishnan A, Bashir ST, et al. Effect of different adjuvants on the longevity and strength of humoral and cellular immune responses to the HCV envelope glycoproteins. *Vaccines (Basel)*. 2019;7. doi:10.3390/vaccines7030071.
16. Krishnan L, Dicaire CJ, Patel GB, Sprott GD. Archaeosome vaccine adjuvants induce strong humoral, cell-mediated, and memory responses: comparison to conventional liposomes and alum. *Infect Immunol*. 2000;68:54–63. doi:10.1128/IAI.68.1.54-63.2000.
17. Sprott GD, Yeung A, Dicaire CJ, Yu SH, Whitfield DM. Synthetic archaeosome vaccines containing triglycosylarchaeols can provide additive and long-lasting immune responses that are enhanced by archaetidylserine. *Archaea*. 2012;2012:513231. doi:10.1155/2012/513231.
18. Gurnani K, Kennedy J, Sad S, Sprott GD, Krishnan L. Phosphatidylserine receptor-mediated recognition of archaeosome adjuvant promotes endocytosis and MHC class I cross-presentation of the entrapped antigen by phagosome-to-cytosol transport and classical processing. *J Immunol*. 2004;173:566–78. doi:10.4049/jimmunol.173.1.566.
19. Sprott GD, Sad S, Fleming LP, Dicaire CJ, Patel GB, Krishnan L. Archaeosomes varying in lipid composition differ in receptor-mediated endocytosis and differentially adjuvant immune responses to entrapped antigen. *Archaea*. 2003;1:151–64. doi:10.1155/2003/569283.
20. Patel R, Kim K, Shutinoski B, Wachholz K, Krishnan L, Sad S. Culling of APCs by inflammatory cell death pathways restricts TIM3 and PD-1 expression and promotes the survival of primed CD8 T cells. *Cell Death Differ*. 2017;24:1900–11. doi:10.1038/cdd.2017.112.
21. Gu BJ, Sun C, Fuller S, Skarratt KK, Petrou S, Wiley JS. A quantitative method for measuring innate phagocytosis by human monocytes using real-time flow cytometry. *Cytometry A*. 2014;85:313–21. doi:10.1002/cyto.a.22400.
22. Clarke SR, Barnden M, Kurts C, Carbone FR, Miller JF, Heath WR. Characterization of the ovalbumin-specific TCR transgenic line OT-I: MHC elements for positive and negative selection. *Immunol Cell Biol*. 2000;78:110–17. doi:10.1046/j.1440-1711.2000.00889.x.
23. Cruse JM, Lewis RE, Wang H, Schreuder GM, Marsh SG, Kennedy LJ. 7 - Antigen Presentation. In: Cruse JM, Lewis RE, Wang H, editors. *Immunology guidebook*. Cambridge, MA: Elsevier Academic Press; 2004. p. 267–76. doi:10.1016/B978-012198382-6/50031-5.
24. Marichal T, Ohata K, Bedoret D, Mesnil C, Sabatel C, Kobiyama K, Lekeux P, Coban C, Akira S, Ishii KJ, et al. DNA released from dying host cells mediates aluminum adjuvant activity. *Nat. Med*. 2011;17:996–1002. doi:10.1038/nm.2403.
25. Kono H, Rock KL. How dying cells alert the immune system to danger. *Nat Rev Immunol*. 2008;8:279–89. doi:10.1038/nri2215.
26. Coler RN, Bertholet S, Moutaftsi M, Guderian JA, Windish HP, Baldwin SL, Laughlin EM, Duthie MS, Fox CB, Carter D, et al. Development and characterization of synthetic glucopyranosyl lipid adjuvant system as a vaccine adjuvant. *PLoS ONE*. 2011;6(1):e16333. doi:10.1371/journal.pone.0016333.
27. Lambert SL, Yang CF, Liu Z, Sweetwood R, Zhao J, Cheng L, Jin H, Woo J. Molecular and cellular response profiles induced by the TLR4 agonist-based adjuvant glucopyranosyl lipid A. *PLoS One*. 2012;7:e51618. doi:10.1371/journal.pone.0051618.
28. Chilton PM, Embry CA, Mitchell TC. Effects of differences in lipid A structure on TLR4 pro-inflammatory signaling and inflammasome activation. *Front Immunol*. 2012;3:154. doi:10.3389/fimmu.2012.00154.
29. Tolson DL, Latta RK, Patel GB, Sprott GD. Uptake of archaeobacterial liposomes and conventional liposomes by phagocytic cells. *J Liposome Res*. 1996;6:755–76. doi:10.3109/08982109609039925.
30. Pozzi LA, Maciaszek JW, Rock KL. Both dendritic cells and macrophages can stimulate naive CD8 T cells in vivo to proliferate, develop effector function, and differentiate into memory cells. *J Immunol*. 2005;175:2071–81. doi:10.4049/jimmunol.175.4.2071.
31. Roche PA, Cresswell P. Antigen processing and presentation mechanisms in myeloid cells. *Microbiol Spectr*. 2016;4(3). doi:10.1128/microbiolspec.MCHD-0008-2015.
32. Savina A, Amigorena S. Phagocytosis and antigen presentation in dendritic cells. *Immunol Rev*. 2007;219:143–56. doi:10.1111/j.1600-065X.2007.00552.x.
33. Delamarre L, Pack M, Chang H, Mellman I, Trombetta ES. Differential lysosomal proteolysis in antigen-presenting cells determines antigen fate. *Science*. 2005;307:1630–34. doi:10.1126/science.1108003.
34. Lennon-Dumenil AM, Bakker AH, Maehr R, Fiebiger E, Overkleeft HS, Roseblatt M, Ploegh HL, Lagaudrière-Gesbert C. Analysis of protease activity in live antigen-presenting cells shows regulation of the phagosomal proteolytic contents during dendritic cell activation. *J. Exp. Med*. 2002;196:529–40. doi:10.1084/jem.20020327.
35. Wolf M, Greenberg PD. Antigen-specific activation and cytokine-facilitated expansion of naive, human CD8+ T cells. *Nat Protoc*. 2014;9:950–66. doi:10.1038/nprot.2014.064.
36. Topham DJ, Reilly EC. Tissue-resident memory CD8(+) T cells: from phenotype to function. *Front Immunol*. 2018;9:515. doi:10.3389/fimmu.2018.00515.
37. Berg RE, Cordes CJ, Forman J. Contribution of CD8+ T cells to innate immunity: IFN-gamma secretion induced by IL-12 and IL-18. *Eur J Immunol*. 2002;32:2807–16. doi:10.1002/1521-4141-(2002010)32:10<2807::AID-IMMU2807>3.0.CO;2-0.
38. Shaw AC, Goldstein DR, Montgomery RR. Age-dependent dysregulation of innate immunity. *Nat Rev Immunol*. 2013;13:875–87. doi:10.1038/nri3547.
39. Bigley V, Barge D, Collin M. Dendritic cell analysis in primary immunodeficiency. *Curr Opin Allergy Clin Immunol*. 2016;16:530–40. doi:10.1097/ACI.0000000000000322.
40. Das M, Kaveri SV, Bayry J. Cross-presentation of antigens by dendritic cells: role of autophagy. *Oncotarget*. 2015;6:28527–28. doi:10.18632/oncotarget.5268.